Comparative Study of the Gas-Phase Bond Strengths of CO_2 and N_2O with the Halide Ions

Kenzo Hiraoka, Kazuo Aruga, and Susumu Fujimaki
Faculty of Engineering, Yamanashi University, Takeda-4, Kofu 400, Japan

Shinichi Yamabe
Department of Chemistry, Nara University of Education, Takabatake-cho, Nara 630, Japan

Thermodynamic data, $\Delta H^\circ_{n-1,n}$ and $\Delta S^\circ_{n-1,n}$, for clustering reactions of halide ions X^- (X = F, Cl, Br, and I) with N_2O were measured with a pulsed electron beam high-pressure mass spectrometer. In contrast to the fact that CO_2 forms a covalent bond with the fluoride ion to yield the fluoroformate ion, FCO_2^-, the interaction between F^- and N_2O is mainly electrostatic. It was found that the cluster ions $F^-(N_2O)_n$ complete the first shell at $n = 6$, thus forming an octahedral structure. The difference between $F—CO_2^-$ and $F^- \cdots N_2O$ is discussed in terms of Coulombic, exchange, and charge-transfer interactions. The $X^-(N_2O)_2$ clusters (X = Cl, Br and I) are found to be of C_{2h} symmetry, while $F^-(N_2O)_2$ is of a twisted form and is slightly asymmetric due to a slight participation of covalency (charge transfer) in the core ion $F^- \cdots N_2O$. *(J Am Soc Mass Spectrom 1993, 4, 58–64)*

Carbon dioxide (CO_2) and nitrous oxide (N_2O) are isoelectronic molecules and are linear according to Walsh's rule [1]. However, their electronic structures are entirely different. While CO_2 is composed of π, $\bar{\pi}$, and σ bonds, N_2O is described as $N_2 \rightarrow O$, that is, a nitrogen molecule coordinated to an oxygen atom.

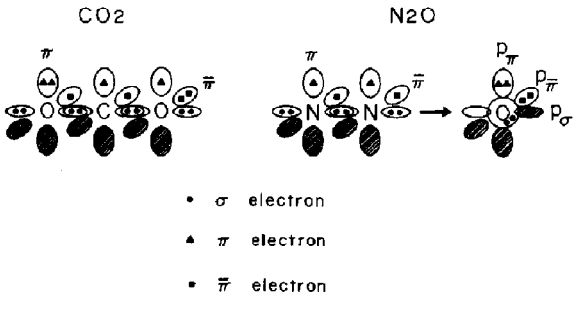

CO_2 is a symmetric nondipolar molecule with a large quadrupole moment ($Q = -4.4 \times 10^{-26}$ cgs esu). N_2O is slightly dipolar (dipole moment $\mu = 0.17$ D) and has a somewhat smaller quadrupole moment ($Q = -3.0 \times 10^{-26}$ cgs esu) [2] than CO_2. These differences in electronic properties tempted us to compare the bond strengths of CO_2 and N_2O with halide ions. In our previous work [3], thermochemical data, $\Delta H^\circ_{n-1,n}$ and $\Delta S^\circ_{n-1,n}$, for the clustering reaction 1 (X = F, Cl, Br, and I) were reported.

$$X^-(CO_2)_{n-1} + CO_2 = X^-(CO_2)_n \qquad (1)$$

The large value of $-\Delta H^\circ_{0,1}$ (32.3 kcal/mol) and a sudden decrease of $-\Delta H^\circ_{1,2}$ (7.3 kcal/mol) for reaction 1 with X = F indicate that the core ion is not $F^- \cdots CO_2$, but rather FCO_2^-, the fluoroformate ion. Ab initio molecular orbital (MO) calculations revealed that the two oxygen atoms on the formate anion are the best targets for the solvent CO_2. These two O atoms are capable of accepting four CO_2 molecules as ligands. The F atom in the FCO_2^- core ion is found to be a poorer attractive site and can accommodate only the sixth CO_2. That is, the ion center is switched from F to O through FCO_2^- formation. In contrast to the case of FCO_2^-, the bonding of Cl^-, Br^-, and I^- to CO_2 molecules is found to be mainly electrostatic, and the most symmetric structures are formed for $X^-(CO_2)_n$ (X = Cl, Br, and I).

In this work, $\Delta H^\circ_{n-1,n}$ and $\Delta S^\circ_{n-1,n}$ for reaction 2 (X = F, Cl, Br, and I) were measured.

$$X^-(N_2O)_{n-1} + N_2O = X^-(N_2O)_n \qquad (2)$$

Ab initio MO calculations were also made to examine the similarity or the difference in the bonding pattern between $X^- \cdots CO_2$ and $X^- \cdots N_2O$.

Address reprint requests to Kenzo Hiraoka, Faculty of Engineering, Yamanashi University, Takeda-4, Kofu 400, Japan.

1044–0305/93/$5.00

Received March 20, 1992
Revised June 30, 1992
Accepted June 30, 1992

Experimental and Theoretical Methods

The experiments were made with a pulsed electron beam high-pressure mass spectrometer. The general experimental procedures were similar to those described in our previous paper [3]. Briefly, the major gas N_2O was purified by passing it through a dry ice–acetone cooled 3A molecular sieve trap. Electron capture agents NF_3, CCl_4, CH_2Br_2, and CH_3I, producing ions F^-, Cl^-, Br^-, and I^-, respectively, were introduced into 0.5–3 torr of N_2O major gas through a flow-controlling stainless steel capillary. The pressures of NF_3, CCl_4, CH_2Br_2, and CH_3I introduced into the N_2O carrier gas were $\simeq 10$, $\simeq 1$, 10^{-2} and $\simeq 1$ mtorr, respectively. With decrease of the ion source temperature, charging of the ion source was observed below 133, 172, 161, and 145 K for the measurement of X = F, Cl, Br, and I, respectively. Because the condensation temperature of a few torr of N_2O is ~ 130 K, the charging of the ion source was likely to be due to the condensation of the electron capture agent gases on the inner surface of the cold ion source. With charging of the ion source, the equilibria of the clustering reactions could not be observed. The measurements of the equilibrium constants for reaction 2 were made just before charging of the ion source began.

In addition to the $X^-(N_2O)_n$ ions, the cluster ions $O^-(N_2O)_n$ and $NO^-(N_2O)_n$ originated from the major gas N_2O were also observed. The relative intensities of $O^-(N_2O)_n$ and $NO^-(N_2O)_n$ were much weaker than those of $X^-(N_2O)_n$. This indicates that the cross section of the dissociative electron capture reaction for N_2O is considerably smaller than those for the electron capture agents, NF_3, CCl_4, CH_2Br_2, and CH_3I.

Structures of $X^-(N_2O)_n$ ($n = 1$ and 2) are fully optimized with ab initio MO calculations of 6 − 31 + G (X = F and Cl only) and 3 − 21 + G basis sets (+ means a diffuse *sp* orbital on all atoms). The orbital exponents are 0.0639(N), 0.0845(O), 0.1076(F), 0.0483(Cl), 0.060(Br), and 0.054(I), respectively. Exponents of Br and I are obtained by minimizing total energies of bromide and iodide ions. Other exponents (of N, O, F, and Cl) are taken from the literature [4]. All the ab initio calculations are performed using the GAUSSIAN 90 [5] program installed at the CONVEX C-220 computer. Except for the 3 − 21G basis set of Br and I [6], basis sets are those implemented in the GAUSSIAN 90 program.

Experimental Results

Figure 1 represents the temporal profiles of $F^-(N_2O)_n$ with $n = 2$–5 in 2.81 torr N_2O and 13 mtorr NF_3 at 199.2 K. The equilibria are seen to be established shortly after the electron pulse. This was also the case for X = Cl, Br, and I. The results for the experimentally measured equilibrium constants for reactions 2 are displayed in the van't Hoff plots in Figure 2. In Table 1, the enthalpy and entropy changes obtained from Figure 2 are summarized, together with those for reactions 1 taken from our previous work [3]. In Figure 3, the $-\Delta H^\circ_{n-1,n}$ values for reactions 1 and 2 are shown as a function of n.

In Figure 3, the values of $-\Delta H^\circ_{n-1,n}$ for reactions 2 decrease only gradually with n, indicating that the interactions between the core ions and the ligand N_2O molecules are mainly electrostatic for all the cases of X = F, Cl, Br, and I. For X = F, a remarkable difference of the bond energy between $-H^\circ_{0,1}(F^-CO_2) = 32.3$ kcal/mol and $-\Delta H^\circ_{0,1}(F^-N_2O) = 9.87$ kcal/mol is found. The covalent bond formation in $F—CO_2^-$ is in marked contrast with the mere electrostatic force involved in the $F^-(N_2O)_n$ clusters. A close inspection of Figure 2 reveals that the plots with $n = 1$ and 2 are closer to each other than those with $n = 2$ and 3 for F^- and Cl^- ions. This tendency is more quantitatively shown in Figure 3, where there appear small but noticeable irregular decreases in $-\Delta H^\circ_{n-1,n}$ between $n = 2$ and 3 for X = F, Cl, and also Br. This irregular decrease is attributed to the congestion of the ligands around the core ions (i.e., exchange repulsion) as n increases from 2 to 3. A similar trend was observed in the clustering reactions of halide ions (X = Cl, Br, and I) with CH_3CN [7] and CH_3OH [8].

In Figure 2, a large gap is observed in the van't Hoff plots for F^- between $n = 6$ and 7 and is clearly reflected in Figure 3 as an irregular decrease in $-\Delta H^\circ_{n-1,n}$ as n increases from 6 to 7. This suggests the completion of an octahedral shell structure in the cluster $F^-(N_2O)_6$. The shell formation is in contrast to the fact that more than six CH_3CN molecules are accommodated in the first shells of $X^-(CH_3CN)_n$ for X = Cl, Br, and I [7]. In the clustering reactions of fluoride ion with CO_2 molecules, the shell completion with $n = 6$ was also observed. However, this is due to the highly anisotropic potential energy surface around the fluoroformate core ion FCO_2^-. Because the interac-

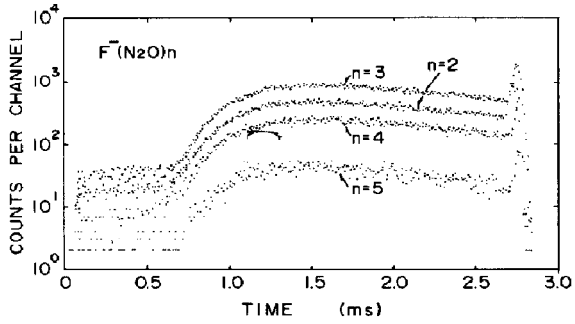

Figure 1. The temporal profiles of ions $F^-(N_2O)_n$ with $n = 2$–5 observed in 2.81 torr N_2O and 13 mtorr NF_3. Ion source temperature = 199.2 K, energy of incident electrons = 2 keV, electron pulse width = 550 μs. At 2.7 ms, a short negative pulse (25 V) is applied to the repeller electrode in the ion source in order to annihilate all ions produced in the ion source. The integration times for the ions $F^-(N_2O)_n$ with $n = 2$–5 are 310, 420, 90, and 180 s, respectively.

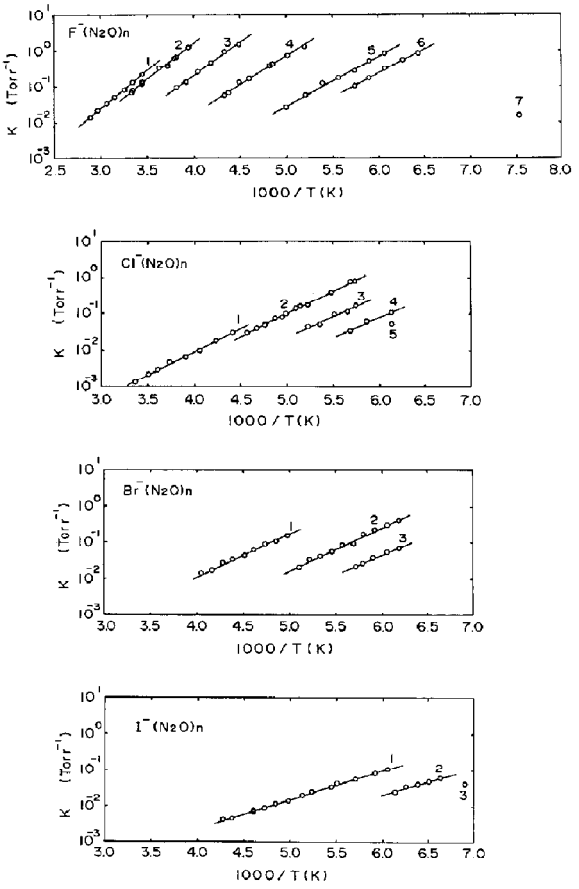

Figure 2. van't Hoff plots of the gas-phase clustering reaction 2, $X^-(N_2O)_{n-1} + N_2O = X^-(N_2O)_n$. Integer numbers in the figure represent values of n.

tion in the cluster $F^-(N_2O)_n$ is mainly electrostatic, the shell completion for $F^-(N_2O)_n$ with $n = 6$ is caused by the exchange repulsion between ligands. The saturation of the first shell with six N_2O ligands is likely to arise from the small size of the core F^- ion (more crowded with smaller n).

In Table 1, the $-\Delta H^\circ_{n-1,n}$ and $-\Delta S^\circ_{n-1,n}$ values for reaction 2 are in the order of $F^- > Cl^- \simeq Br^- > I^-$ with $n \leq 6$. A similar trend was also observed for the clustering reactions of halide ions with many solvent molecules (M) measured in our laboratory, where M = H_2O [7], CH_3CN [7], C_6H_6 [9], C_6F_6 [10, 13] and CO_2 [3]. The values of $-\Delta H^\circ_{n-1,n}$ for X = Cl and Br in Figure 3 are almost degenerate. The similarity of Cl^- and Br^- was discussed in the $X^- \cdots C_6H_6$ complex before [9]. One source is that of physical properties such as the ionic radii (1.67 and 1.82 Å) and polarizabilities (3.5 and 4.8 Å^3). The other source is a critical balance between the charge transfer (CT) and the exchange repulsion (ER) in the clusters X^- (solvent)$_n$ for X = Cl and Br.

In Figure 3, the bond energies of $X^-(CO_2)_n$ are

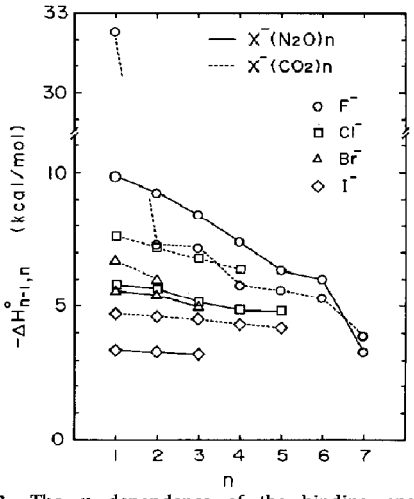

Figure 3. The n dependence of the binding energies of $X^-(N_2O)_{n-1} \cdots N_2O$ together with those of $X^-(CO_2)_{n-1} \cdots CO_2$ taken from ref 3.

greater than those of $X^-(N_2O)_n$ for X = Cl, Br, and I. Because the polarizability of N_2O (α = 2.92 Å^3) is larger than that of CO_2 (α = 2.59 Å^3), the weaker bonds of the N_2O clusters must be due to the difference of the electronic distributions in the N_2O and CO_2 molecules. That is, N_2O provides a less electropositive site than CO_2 toward the halide ions. The detailed theoretical investigation on the nature of bonding of these cluster ions will be given in the following section. The binding energies of $F^-(CO_2)_n$ are smaller than those of $F^-(N_2O)_n$ with n = 2–6. The well-dispersed negative charge in the fluoroformate anion FCO_2^- results in the weaker electrostatic interaction in the subsequent clustering reactions.

The fluoride ion is known to be one of the most aggressive nucleophiles in the gas phase and is found to form very strong bonds with many molecules. In ref 11, one finds that most cluster ions $F^- \cdots M$ (M: ligand molecule) have bond energies larger than 30 kcal/mol. There are few cluster ions $F^- \cdots M$ known with bond energies less than 20 kcal/mol; these are $F^- \cdots Xe$ (6.5 kcal/mol) [12] and $F^- \cdots C_6H_6$ (15.3 kcal/mol) [13]. The present bond energy of $F^- \cdots N_2O$, 9.87 kcal/mol, thus gives another example of an exceptionally small value for a F^- cluster. It is apparent that the N_2O molecule is a very poor Lewis acid. The covalent bond strength in the cluster ion is mainly determined by two opposing factors, namely energy stabilization by electron delocalization and energy destabilization by overlap of the electron clouds between the reactant species (i.e., exchange repulsion). In the case of the formation of the fluoroformate ion FCO_2^-, the energy destabilization by exchange repulsion is overcompensated by formation of the strong F—C bond [3]. In contrast, charge dispersal in $(F—N_2O)^-$ does not take place because formation of the relatively weak N—F bond

Table 1. Thermochemical data, $\Delta H^\circ_{n-1,n}$ in kcal/mol and $\Delta S^\circ_{n-1,n}$ in cal/mol · K, of the gas-phase clustering reactions $X^-(CO_2)_{n-1} + CO_2 = X^-(CO_2)_n$ and $X^-(N_2O)_{n-1} + N_2O = X^-(N_2O)_n$ (X = F, Cl, Br, and I).[a]

	X = F				X = Cl				X = Br				X = I			
	$-\Delta H^\circ_{n-1,n}$		$-\Delta S^\circ_{n-1,n}$		$-\Delta H^\circ_{n-1,n}$		$-\Delta S^\circ_{n-1,n}$		$-\Delta H^\circ_{n-1,n}$		$-\Delta S^\circ_{n-1,n}$		$-\Delta H^\circ_{n-1,n}$		$-\Delta S^\circ_{n-1,n}$	
$(n-1,n)$	CO_2	N_2O	CO_2	N_2O	CO_2	N_2O	CO_2	N_2O	CO_2	N_2O	CO_2	N_2O	CO_2	N_2O	CO_2	N_2O
(0, 1)	32.3	9.87 10.60 (10.39)	26.7	23.9	7.6	5.79 6.36 (5.20)	18.2	19.2	6.7	5.57 5.41	16.5	18.1	4.7	3.78 4.47	13.4	14.1
(1, 2)	7.3	9.23 10.62 (10.29)	18.2	22.7	7.2	5.63 6.53 (5.18)	20.8	19.5	6.0	5.39 5.49	19.0	21.8	4.6	3.30 4.49	17.3	14.2
(2, 3)	7.2	8.42	22.6	23.6	6.8	5.13	22.4	20.0		4.97		22.9	4.5	≃ 3.2	18.4	15[b]
(3, 4)	5.8	7.40	20.3	24.4	≃ 6.4	4.85	25[b]	20.9					4.3		19.0	
(4, 5)	5.6	6.33	22.3	25.5		4.8		22[b]					≃ 4.2		19[b]	
(5, 6)	5.3	6.03	22.5	25.8												
(6, 7)	≃ 3.9	3.3	18[b]	20[b]												

[a] Experimental errors for $\Delta H^\circ_{n-1,n}$ and $\Delta S^\circ_{n-1,n}$ may be within ± 0.3 kcal/mol and ± 3 cal/mol · K, respectively. Data for CO_2 reactions are taken from ref 3. Underlined numbers in $\Delta H^\circ_{n-1,n}$ are the computed bond energies with RHF/3-21 + G, and those in parentheses are with RHF/6-31 + G.

[b] Entropy value $\Delta S^\circ_{n-1,n}$ assumed.

cannot counterbalance energy destabilization by the exchange repulsion and thus electrostatic interaction results in the cluster $F^- \cdots N_2O$.

Computational Results

Figure 4 shows the $X^-(N_2O)$ geometry. For X = F, a weak bond with the F ··· N distance 2.6–2.8 Å is confirmed, while the covalent N—F bond length of NF_3 is 1.35 Å. That is, the electronic structure is not $F—N^+(—O^-) = N^-$ but $F^- \cdots N_2O$. However, a slight charge transfer is involved in this cluster ($F^{-1} \rightarrow F^{0.96}$). The well-known ion size difference (F^-:1.19 Å ≪ Cl^-:1.67 Å ≤ Br^-:1.82 Å < I^-:2.06 Å) is reflected in the computed RHF/3 − 21 + G $X^- \cdots$ NNO distances (F^-:2.83 Å ≪ Cl^-:3.63 Å ≤ Br^-:3.87 Å < I^-:4.25 Å). Noteworthy is the change in the XNO angle (114.9°(F) → 117.3°(Cl) → 118.3°(Br) → 120.1°(I)). This change originates from the difference of the $X^- \cdots O$ exchange repulsion. The larger lobe of X^- overlaps more with the oxygen orbital. To diminish this overlap repulsion, the $X^- \cdots O$ distance becomes enlarged as the size of X^-. In Figure 5, the $X^-(N_2O)_2$ geometry is displayed. The $F^-(N_2O)_2$ is found to be of a twisted and somewhat asymmetric form. In general, the electrostatic interaction results in the symmetric C_{2h} structure for $n = 2$. The C_{2h} of $F^-(N_2O)_2$ is computed to be about 0.2 kcal/mol less stable than this twist geometry. Probably a slight through-space O ··· O overlap repulsion is present and is avoided by the twisting.

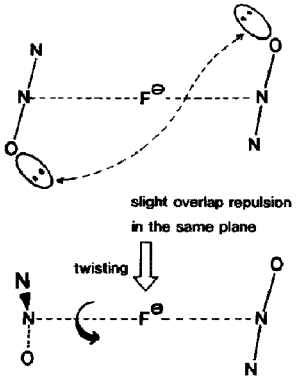

For other $X^-(N_2O)_2$ species, the oxygen–oxygen distances are large enough for the overlap to vanish, leading to planar geometries. Also, the slight distance nonequivalence in $F^-(N_2O)_2$ comes from the small $F^- \cdots N$ covalency. The $n = 2$ clusters other than $F^-(N_2O)_2$ are calculated to be close to C_{2h} symmetry because of the Coulombic force.

The difference of the interaction between $X^- \cdots CO_2$ and $X^- \cdots N_2O$ is analyzed in terms of electronic structures of CO_2 and N_2O. Figure 6 shows atomic net charges and π MOs of two neutral molecules. Since the four geometries of $X^-(N_2O)_1$ in Figure 4 arise mainly from electrostatic forces, the Coulomb energies

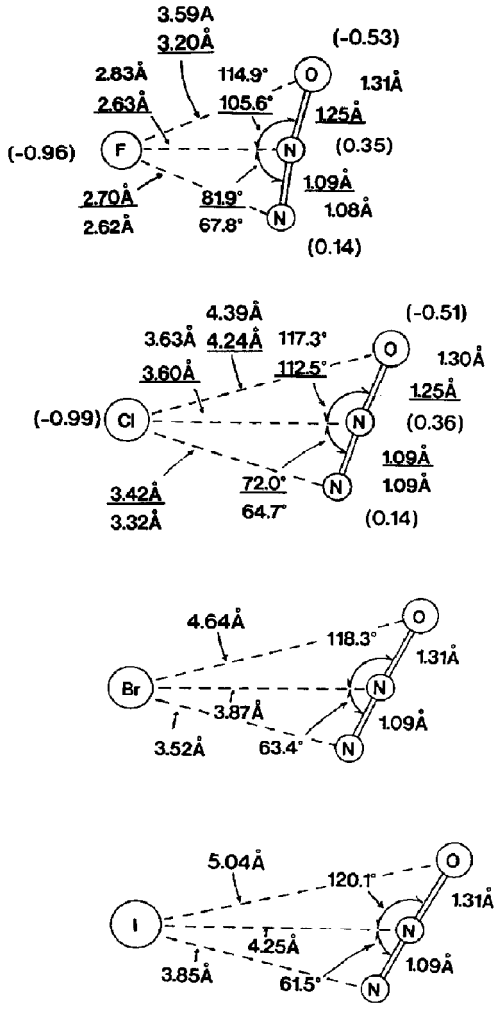

Figure 4. Geometries of $X^-(N_2O)_1$ optimized with RHF/3 − 21 + G (and RHF/6 − 31 + G for X = F and Cl underlined). The N—N distance is 1.09 Å (1.10 Å and exptl. [14] 1.13 Å) and the N—O distance is 1.29 Å (1.24 Å and exptl. 1.18 Å) in the free N_2O molecule. Values in parentheses for X = F and Cl denote Mulliken atomic net charges of 6 − 31G. Because basis sets including diffuse functions (e.g., 3 − 21 + G) tend to give unreasonable charges, the 6 − 31 + G data are adopted.

E_C are estimated roughly by the use of these net charges:

$$E_C(X^- \cdots ABC) = \sum_{\alpha=1}^{3} \frac{(-1)M_\alpha}{R_{X^- - \alpha}}(627.52).$$

Here, α is the A, B, or C atom in the molecule ABC. (−1) is the charge on X^-, and M_α is the net charge on the αth atom. $R_{X^- - \alpha}$ is the interatomic distance in atomic units (1 a.u. = 0.5292 Å). The energy in atomic units can be converted to that in kcal/mol through 1 a.u. = 627.52 kcal/mol. As an example, $E_C(F^- \cdots N_2O)$ is given below.

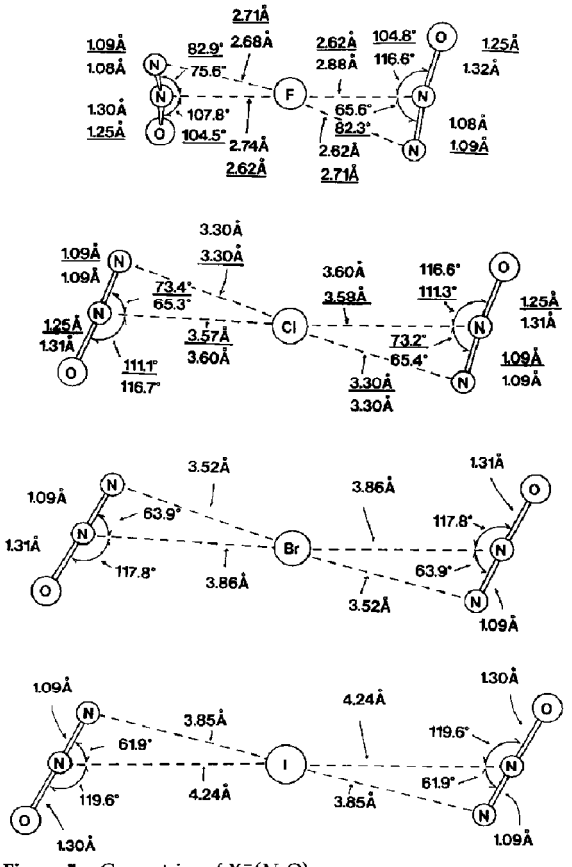

Figure 5. Geometries of $X^-(N_2O)_2$.

$$E_C(F^- \cdots N_2O)$$

$$= \left[\frac{(-1)(-0.5)}{\underset{0.5292}{\overset{F^- \cdots O}{3.590}}} + \frac{(-1)(+0.40)}{\underset{0.5292}{\overset{F^- \cdots N}{2.833}}} + \frac{(-1)(+0.10)}{\underset{0.5292}{\overset{F^- \cdots N}{2.624}}} \right] 627.52$$

$$= -13.29 \text{ kcal/mol}$$

This Coulomb stabilizing energy is derived from the RHF/6 − 31G charge. With RHF/6 − 31G*, $E_C(F^- \cdots N_2O) = -13.35$ kcal/mol is obtained, which indicates that the energy E_C is essentially independent of computational method. $-E_C(F^- \cdots N_2O) \simeq 13$ kcal/mol is larger than the observed $-\Delta H^\circ_{0,1} = 9.87$ kcal/mol for $F^-(N_2O)_n$. Similar calculations of $E_C(Cl^- \cdots N_2O)$ are made, and the same trend, $-E_C(Cl^- \cdots N_2O) = 8.75$ kcal/mol > $-\Delta H^\circ_{0,1} = 5.79$ kcal/mol for $Cl^-(N_2O)_n$ is found as in $F^- \cdots N_2O$. On the other hand, $-E_C(Cl^- \cdots CO_2)$ is calculated by the use of the

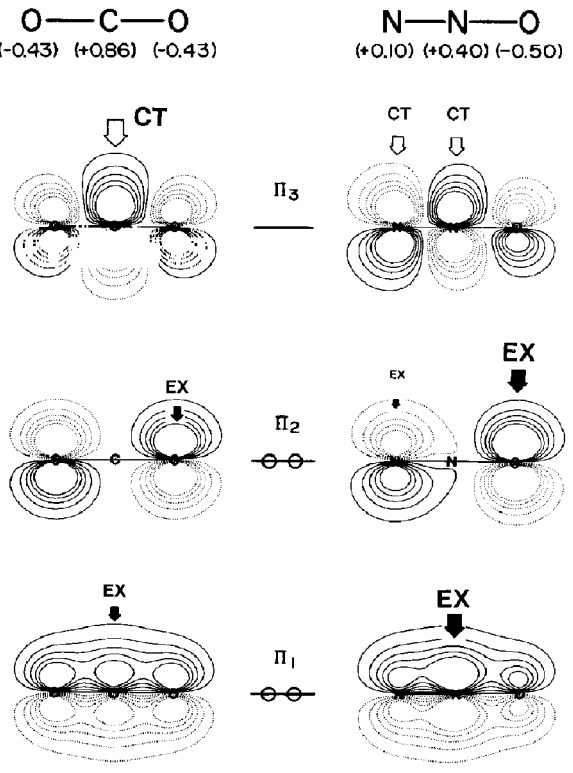

Figure 6. The 6 − 31 + G atomic net charges shown in parentheses of CO_2 and N_2O. Three π MOs of CO_2 and N_2O are also drawn, where π_1 and π_2 are occupied orbitals and π_3 is a vacant one. CT expressed by the bold outline arrow is the charge transfer from a halide ion. EX for π_2 denoted by the solid black arrow is the exchange repulsion against the electronic charge of the ion.

geometry reported previously [3] and is 8.33 kcal/mol, which is closer to $-\Delta H^\circ_{0,1} = 7.6$ kcal/mol of $Cl^-(CO_2)_n$ [3]. Compare

$$-E_C = 8.75 \text{ kcal/mol} > -\Delta H^\circ_{0,1} = 5.79 \text{ kcal/mol}$$

for $Cl^- \cdots N_2O$ with

$$-E_C = 8.33 \text{ kcal/mol} \simeq -\Delta H^\circ_{0,1} = 7.6 \text{ kcal/mol}$$

for $Cl^- \cdots CO_2$.

By these calculations of E_C values, we have obtained two important results: (1) Electrostatic energies are similar in $Cl^- \cdots N_2O$ and $Cl^- \cdots CO_2$, −8.75 and −8.33 kcal/mol. (2) In the $Cl^- \cdots CO_2$ cluster, the second-order terms in the perturbation formulation, the exchange repulsion (EX) and the charge transfer (CT) almost cancel each other out, leading to $E_C \simeq \Delta H^\circ_{0,1}$. On the other hand, the result $-E_C > -\Delta H^\circ_{0,1}$ for $Cl^- \cdots N_2O$ as well as for $F^- \cdots N_2O$ demonstrates that the EX term predominates over the CT term. Thus, the next concern is with the orbital shapes for the EX and CT terms of CO_2 and N_2O in Figure 6. The vacant MO, π_3, shows clearly that the carbon atom of CO_2 is a better target than the nitrogen atoms of N_2O for CT from X^-. The π_2 orbital of N_2O representing the p_π lone-pair electrons on the oxygen atom is the source for the $X^- \cdots O$ exchange repulsion. In π_1, the orbital extension on the central nitrogen atom of N_2O is larger than that on the carbon atom of CO_2, which gives rise to the differential extent of the exchange repulsion. Examining the shapes of π MOs of CO_2 and N_2O, we have found that the central carbon atom of CO_2 is a much better reactive center for large CT and small EX than either nitrogen atom of N_2O. The contrast between the one-center attractive site in CO_2 and the poor reactive sites in N_2O is reflected in the difference between the good cancellation of EX and CT in $Cl^- \cdots CO_2$ and EX > CT in $Cl^- \cdots N_2O$. Thus, the binding energy of $Cl^- \cdots N_2O$, 5.79 kcal/mol, smaller than that of $Cl^- \cdots CO_2$, 7.6 kcal/mol, is ascribed to that difference.

For $n = 1$, a geometric isomer X—N = N—O^- is conceivable in view of the X—N covalency and of the following resonance structures:

$$X—N = N—O^- \leftrightarrow X—N^-—N = O$$

For X = F, a planar equilibrium geometry is obtained with both 3 − 21 + G and 6 − 31 + G basis sets.

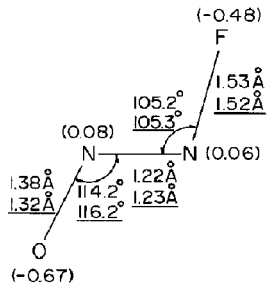

However, this species is computed to be 17.2 kcal/mol (21.6 kcal/mol) less stable than the $F^- \cdots N_2O$ cluster in Figure 4. The instability of the F—N = N—O^- species comes from the small F—N binding energy (= 56 kcal/mol for F—NO) and the odd N—O^- electronic distribution. As shown in the introduction, the terminal nitrogen of the N_2O species is basically the same as that of the nitrogen molecule. Its lone-pair electrons reject the tight covalent linkage with F^-. For X = Cl, Br, and I, the X—N = N—O^- species are calculated as not being formed. The X—N = N—O^- type geometry (X = Cl, Br, and I) is found to be converted to $X^- \cdots N_2O$ during optimization.

In Table 1, computed underlined energies are in good agreement with the experimental values of $-\Delta H^\circ_{n-1,n}$. One problem with the 3 − 21 + G calculation was found. The energy decay as the size n increases was not reproduced (e.g., 10.60 kcal/mol with $n = 1 \rightarrow 10.62$ kcal/mol with $n = 2$ for X = F), which is probably due to a small imbalance between 3 − 21 + G and augmented diffuse orbitals.

Concluding Remarks

In this work, the stability and structure of the $X^-(N_2O)_n$ clusters have been investigated. In view of the large bond energy, 32.3 kcal/mol, of $F^-—CO_2$ [3] and the $N^{\delta+}–O^{\delta-}$ polarization, it was expected that a $F—N^+(—O^-) = N^-$-type cluster is readily formed. However, the $F^- \cdots N_2O$ bond is weak with a 9.87 kcal/mol bond energy and is almost purely electrostatic. This seems to be the first example in which the strong gas phase nucleophile F^- cannot form a covalent bond with first-row atoms in spite of the hard–hard combination. The extent of the cancellation of EX and CT terms leads to the difference of binding energies, namely $-\delta H^\circ_{0,1}(Cl^- \cdots CO_2) > -\Delta H^\circ_{0,1}(Cl^- \cdots N_2O)$.

Acknowledgments

We express our appreciation for the financial support of the Morino Foundation for Molecular Science and the grant in aid from the Japanese Ministry of Education (in part on Priority Area "Theory of Chemical Reactions"). We also thank the Information Processing Center of Nara University of Education for the allotment of the CPU time of the CONVEX C-220 computer.

References

1. Walsh, A. D. *J. Chem. Soc.* **1953**, 2260.
2. Stogryn, D. E.; Stogryn, A. P. *Molec. Phys.* **1966**, *11*, 371.
3. Hiraoka, K.; Mizuse, S.; Yamabe, S. *J. Chem. Phys.* **1987**, *87*, 3647.
4. Clark, T.; Chandrasekhar, J.; Spitznagel, G. W.; Schleyer, P. v. R. *J. Comput. Chem.* **1983**, *4*, 294.
5. Frisch, M. J.; Head-Gordon, M.; Trucks, G. W.; Foresman, J. B.; Schlegel, H. B.; Raghavachari, K.; Robb, M. A.; Binkley, J. S.; Gonzalez, C.; DeFrees, D. J.; Fox, D. J.; Whiteside, R. A.; Seeger, R.; Melius, C. F.; Baker, J.; Martin, R. L.; Kahn, L. R.; Stewart, J. J. P.; Topiol, S.; Pople, J. A. GAUSSIAN 90, Revision F; Gaussian, Inc.: Pittsburgh, PA, 1990.
6. Dobbs, K. D.; Hehre, W. J. *J. Comput. Chem.* **1986**, *7*, 359.
7. Hiraoka, K.; Mizuse, S.; Yamabe, S. *J. Phys. Chem.* **1988**, *92*, 3943.
8. Hiraoka, K.; Yamabe, S. *Int. J. Mass Spectrom. Ion Process.* **1991**, *109*, 133.
9. Hiraoka, K.; Mizuse, S.; Yamabe, S. *Chem. Phys. Lett.* **1988**, *147*, 174.
10. Hiraoka, K.; Mizuse, S.; Yamabe, S. *J. Phys. Chem.* **1987**, *91*, 5294.
11. Keesee, R. G.; Castleman, A. W. Jr. *J. Phys. Chem. Ref. Data* **1986**, *15*, 1011.
12. De Vreugd, C.; Wijnaendts Van Resandt, R. W.; Los, J. *Chem. Phys. Lett.* **1979**, *65*, 93.
13. Hiraoka, K.; Mizuse, S., Yamabe, S. *J. Chem. Phys.* **1987**, *86*, 4102.
14. Watson, J. K. G. *J. Mol. Spectry.* **1973**, *48*, 479.